ARTICLE NO. 79-0043R

C80-005

Three-Dimensional Shock Structures for Transonic/Supersonic Compressor Rotors

20016
20017

David C. Prince Jr.*
General Electric Co., Cincinnati, Ohio

This paper reviews experience at evaluating three-dimensional shock structures for transonic/supersonic compressor rotors, including experimental results obtained by holography, laser velocimetry, and high-frequency pressure transducers. Typical shock wave angles are oblique to the relative flow with angles in the range 60-65 deg range for maximum deflection, rather than the 40-50 deg range predicted by conventional cascade analyses. Results are partially explained by obliquity of the shocks in between-blade-streamsurfaces. Procedures for generating analytical flow patterns consistent with experiment, including supersonic/subsonic transition through oblique shocks, are demonstrated.

Introduction

MANY investigations into the shock structures of transonic and supersonic compressor rotors can be found in the literature. The various treatments may emphasize analytical[2,7-15] or experimental[1,3-6,12,14,15] techniques. The frustrations of the investigators are sometimes described very clearly:

> "The pressure increase in the normal shock does not agree with the theoretical value of a one-dimensional supersonic flow."[6]

> "It is recognized that the velocity jump across the normal shock does not follow the classical normal shock relations."[5]

> "Considered in two dimensional terms this front would represent a normal shock. . . . In each case, the downstream total pressure obtained in this way was substantially less than the average downstream total pressure taken from blade element data. . . . Even though the flow downstream of the oblique shocks. . . appears to be supersonic, the pressure surface pressure increases when the back pressure is increased. . . . This sort of back pressure influence violates the characteristics of two-dimensional supersonic flows."[1]

> "As seen, many of the contours are normal rather than parallel to the anticipated shock direction. It is evident from these plots that the rotor tip pressure contours do not explicitly define the shock pattern."[4]

Over a period of years this author has been collecting experience to show that the typical shock wave orientation at the leading edges of supersonic compressor rotor tips, with relative upstream Mach numbers in the range 1.4-1.8, is not at 40-45 deg from the pressure surface, as would be predicted from conventional two-dimensional supersonic flow analysis, but rather is in the 60-70 deg range, corresponding roughly to maximum theoretical stream deflection and near-sonic downstream Mach number. Apparently, it is coincidental that this wave orientation usually appears to be perpendicular to the line through airfoil leading edges, within measurement resolution.

Method of Characteristics analyses for two-dimensional supersonic cascades have been reported in Refs. 2, 12, 14, and 17-21. In most cases these analyses deal with cascades in which the flow is supersonic everywhere, except possibly for a small region around the leading edge stagnation point,[12,14,17,20] where the local subsonic zone is simulated by a simple model. Reference 12 presents a favorable comparison between a theoretical wave shape and a two-dimensional cascade test. Reference 19 presents high-frequency casing static pressure measurements showing a passage shock that is significantly rotated from the axial direction. The information in Ref. 19 does not go into detail about the generality of this result or about comparison between the measured discontinuities and the predictions.

Most investigators with serious concern for both supersonic and subsonic properties of cascade flowfields have chosen to use "time-marching" methods.[7-11,16] Reference 14 summarizes the status of these methods in 1973: "In principle the time-marching methods could also be employed for purely subsonic flows. This is unlikely to be economically viable. . . . it appears likely that time-marching will be reserved for cases having supersonic flow and shocks." In his dicussion of Ref. 14, the present author pointed out that two-dimensional, time-marching methods do not seem likely to recognize the possible occurrence of very low-suction surface pressures, or of supersonic pressure surface pressures responding to throttling.

Reference 15 reports on an ambitious program to perform fully three-dimensional analyses of supersonic compressor rotors. The problem of obtaining reasonable resolution with feasible economics seems likely to present serious obstacles to this approach. Reference 22 also deals with the fully three-dimensional flow, restricted to geometries that do not generate oblique shocks. Productive investigations can sometimes be carried out within that restriction, but it is necessary to prove that the configurations are realistic relative to likely applications.

The objectives of this paper are to review some typical experiences on the shock structures of supersonic compressor rotors, and to present a progress report on investigations seeking to reconcile the observations with conventional flow theory.

Presented as Paper 79-0043 at the 17th Aerospace Sciences Meeting, New Orleans, La., Jan. 15-17, 1979; submitted Feb. 13, 1979; revision received June 29, 1979.

Index categories: Supersonic and Hypersonic Flow; Subsonic Flow.

*Consulting Engineer, Advanced Engineering and Technology Programs Dept. Associate Fellow AIAA.

Table 1 Supersonic compressor shock structure features

1)	Wave angles approximate maximum deflection.
2)	Suction surface pressures near the leading edge are below 80% of upstream.
3)	Shock discontinuities are substantially below expectation.
4)	Pressure surface pressures in supersonic passages respond to back pressure.
5)	Passage and downstream shocks disappear at supersonic pressure levels.

Characteristic Features of Supersonic Compressor Rotor Flow Patterns

The most conspicuous features of supersonic compressor shock observations are given in Table 1. This author has had the opportunity to study data from 8 to 10 compressor configurations in considerable detail. An additional half-dozen have contributed some support to the study.

Within the scope of this paper, it has been necessary to choose a few examples to illustrate the elements of Table 1. Apparently not one of the principal investigative techniques, high-frequency response transducers, laser velocimetry, and laser holography, has been developed to the point where it can be used routinely to give 100% reliable results. Different experiments might have been more convincing for any individual element of the pattern. It is believed that the three examples used are representative of the experience, and that the pattern of Table 1 should be useful as a framework for evaluating other investigations.

Shock Structure Example 1—NASA/AiResearch 1600 ft/s Low Loading Transonic Fan Stage

The NASA/AiResearch Transonic Fan Stage[2-4] provided data displaying the shock structure with less dependence on complicated data reduction procedures than any other readily available source. Reference 4 reproduces a selection of hologram photographs of the shock structure in the vehicle under various test conditions. NASA has made original hologram plates available to investigators for independent study. Figure 1 is a composite of photographs made from these plates at the General Electric Co.

This paper assumes that the photographs display the shock structure intersections with the viewing window. Where two adjacent leading-edge shock structures appear, they are used for definition of the leading-edge plane. An enlargement of the hologram for the low back pressure design speed test condition is presented as Fig. 2. This figure includes suggested interpretations of the photographic evidence of the geometry and the wave angles. The angle between the suction surface near the leading edge and the leading-edge plane appears to be within 3 deg of the design intent of Ref. 2, suggesting that distortion from the viewing angle is not serious. A simple two-dimensional wave angle prediction based on the pressure surface metal angle from Ref. 2 is shown, and also a more sophisticated wave prediction using cascade analysis techniques described later in this paper. The sophisticated procedure gives a curved bow wave, at least qualitatively similar to the experimental results in Ref. 23 and the analytical reasoning in Ref. 24. At a reasonable distance from the leading edge, this procedure gives a wave angle consistent with the simple prediction, and conspicuously different from the observation.

An independent confirmation of the wave angle comes from the data from high-frequency response static pressures on the rotor casing. Figure 3 has been adapted from Fig. 25 of Ref. 3 by applying two principal assumptions:

1) The sawtooth appearance of the signals from transducers 8, 9, and 10 is characteristic of low back pressure operation, reflecting re-expansion downstream of a choked throat. This re-expansion diminishes as the back pressure is raised, and would disappear altogether if the passage flow became subsonic throughout. (Presentations in Ref. 1, for example, show this.)

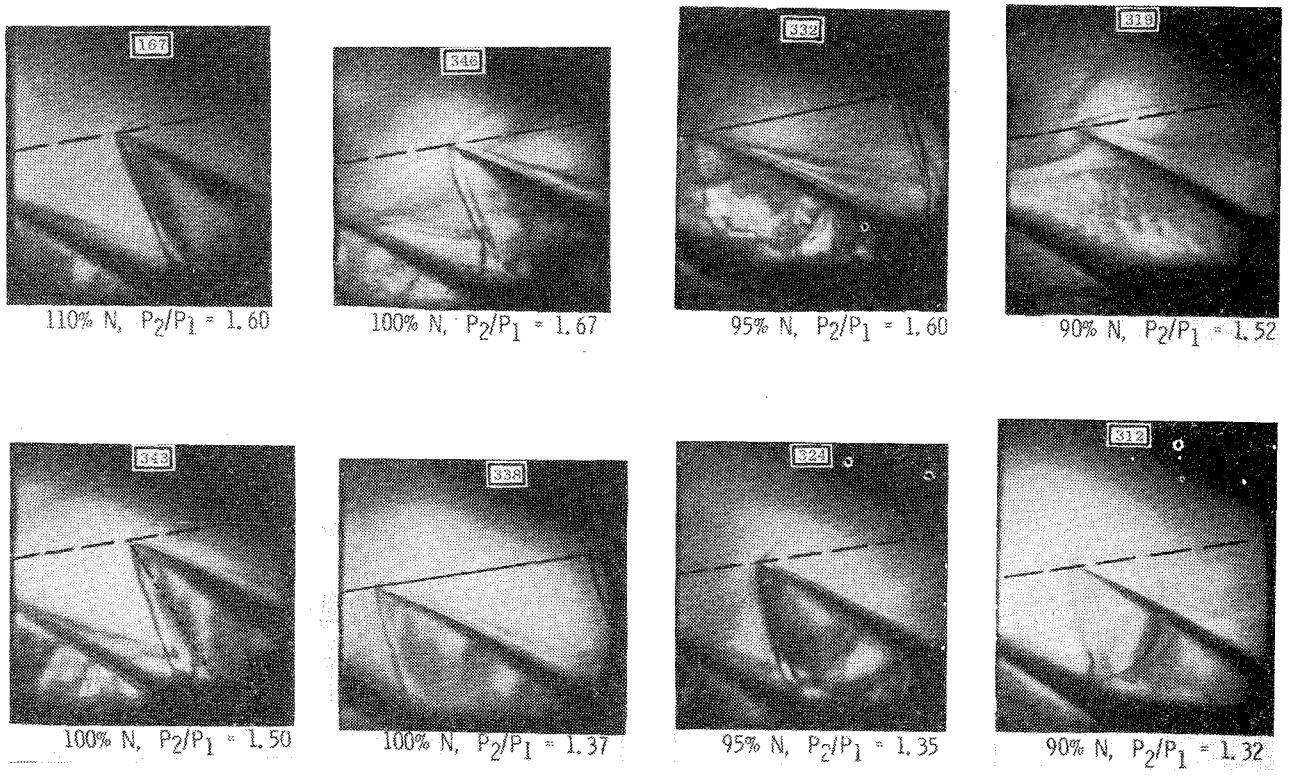

Fig. 1 Hologram representation of blade tip shock structure for transonic compressor rotor—NASA/AiResearch 1600 ft/s low loading transonic fan stage (Ref. 4).

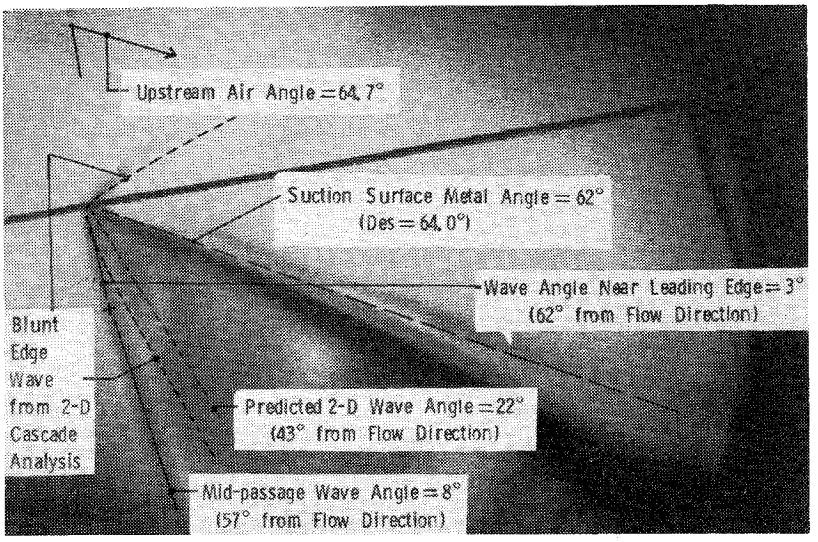

Fig. 2 Enlarged view of hologram showing geometric interpretations. 100% N, $P_2/P_1 = 1.37$.

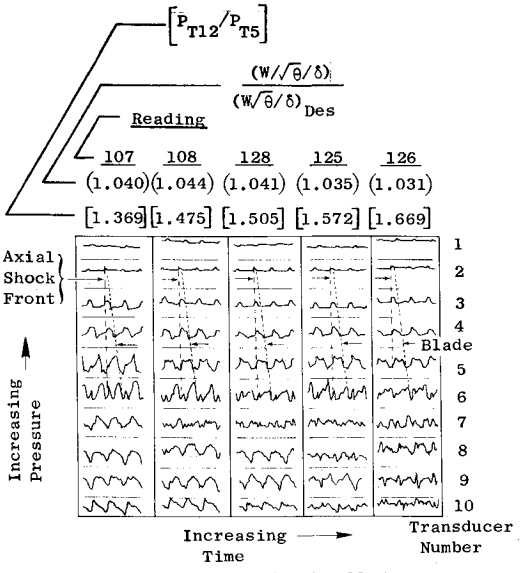

Fig. 3 Typical transducer pressure signals—NASA/AiResearch 1600 ft/s low loading transonic fan stage (adapted from Fig. 25, Ref. 3).

2) Where the characteristics of transducers 1 and 2 show long periods of nearly constant pressure, interrupted by short disturbances, the disturbance is a pressure increase.

These two assumptions lead to a corollary deduction about the time scale which is included in the adaptation. Conspicuous features of Fig. 3 are the time identities of pressure rise signals from transducers 2-6, interpreted as an axial shock front, and progressive phase shifts for pressure drop signals on the same transducers, appropriate for blade passage.

Figure 4 presents the results of processing one of the pressure signal adaptations of Fig. 3 to form a static pressure contour map. The phase relationships among the pressure drop signals in Fig. 3 agreed with the actual blade stagger. Some fidelity in the signals has been sacrificed during successive transcriptions of the data, obscuring the fine details of the leading-edge shock shape. It is clear that the shock pressure rise near the suction surface is substantially upstream of the shock cancellation corner of the design.

This first example has served as an introduction to the opening statement that typical leading-edge shock wave angles for supersonic compressors are in the range of wave angles for maximum deflection or sonic downstream flow. The large wave angle is observed by optical (considering the holograms to be shadowgraphs) means and by casing pressure measurements.

Shock Structure Example 2—General Electric High Tip Speed (550 m/s) High Loading Fan Stage

Wisler[5] reported on using the laser velocimeter (LV) to measure the shock structure of a supersonic fan stage, not only at the blade tip but also at various radial positions within the rotor. A similar investigation is reported in Ref. 6. These two investigations appear to contain the only readily available results of this type.

As mentioned earlier, Wisler observed that the velocity jump observed across a shock "does not follow the classical normal shock relations." A follow-on investigation was undertaken in an attempt at reconciliation. Figure 5 presents a photographic view of the absolute velocity components resulting from the new study. The horizontal scale is defined by the time between passage of successive blades. Axial measurement planes are in inches downstream of the rotor hub leading edge.

On Fig. 5a on the stream surface for 10% flow from the casing, near-stall shock data are shown at almost exactly the same time location for the two axial positions, $Z = 0.88$ and $Z = 1.05$, implying an axial front. Downstream of these two positions the shock appears earlier, making the wave front more nearly normal. At the farthest upstream position, only preshock data were obtained. Considering the time location of the extreme point, the wave angle cannot be more oblique than the axial direction; somewhat more normal is more probable. Using the shock equations to predict velocity discontinuities as functions of the wave angle shows that, for wave angles near axial, the discontinuity in the axial velocity component ought to be related to the wave angle at the rate of 10% for 5 deg—a decrease in axial velocity implies a wave angle toward the normal.

Shock data on the nominal operating line on Fig. 5a also imply an axial shock front, displaced circumferentially (and into cascade passage) by 6% of the blade spacing from the position near-stall. The data suggest that the axial velocity component may increase across the shock front, but not as much as 10%. The data seem incompatible with a shock inclined more than 5 deg to the axial direction and compatible with an axial front followed by re-expansion downstream of the throat.

On Fig. 5b, showing the stream surface for 30% flow from the casing, the time locations for the shock are well defined for both throttle settings and indicate axial orientations. The wave front is displaced circumferentially by 10% of the blade spacing between throttle settings. Discontinuities in the axial component of velocity across the wave front are negligible (on this stream surface, 7% axial velocity change is equivalent to 5 deg change in wave angle).

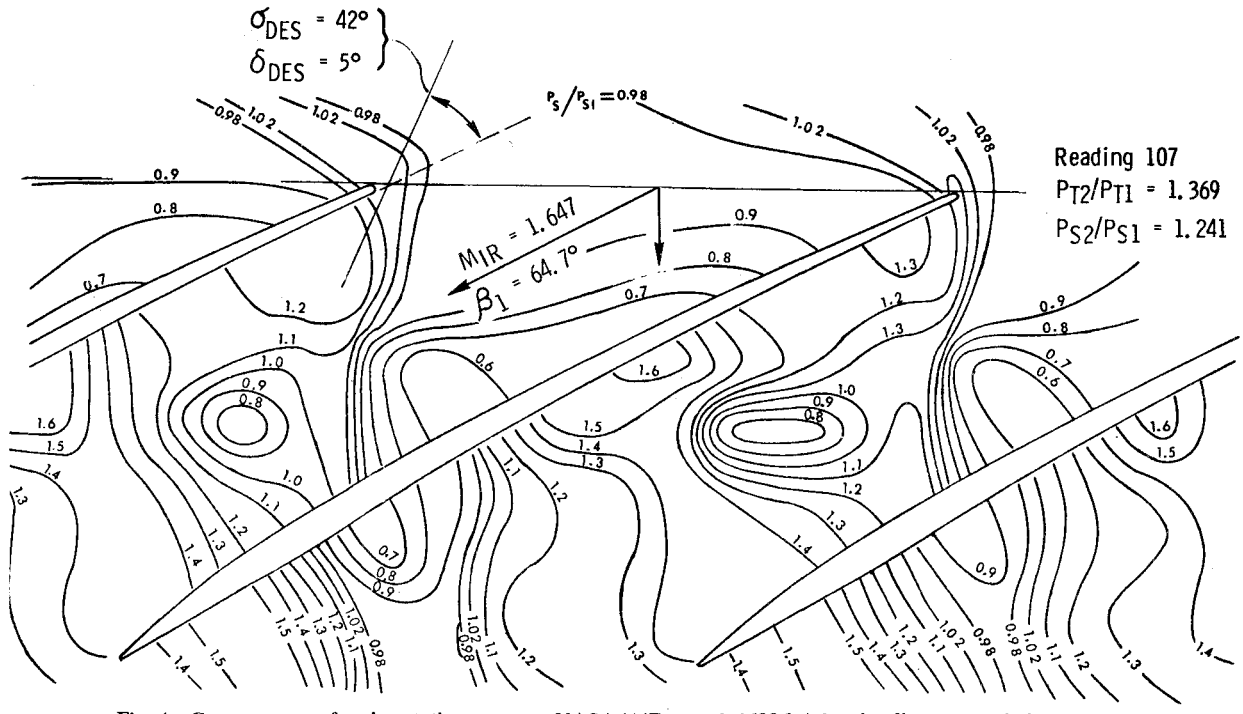

Fig. 4 Contour map of casing static pressure—NASA/AiResearch 1600 ft/s low loading transonic fan stage.

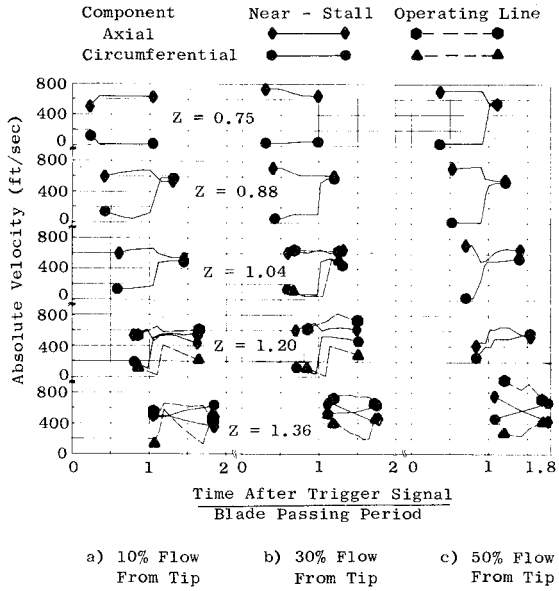

Fig. 5 Absolute velocity components inferred from laser velocimeter measurements—General Electric high tip speed (550 m/s) fan stage.

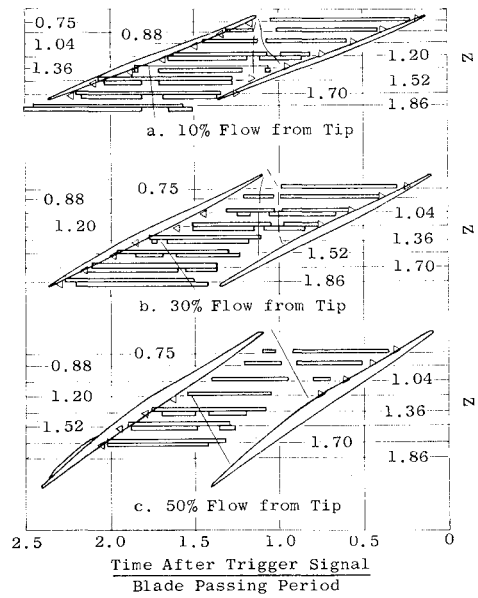

Fig. 6 Shock patterns inferred from laser velocimeter measurements—General Electric high tip speed (550 m/s) fan stage.

Leading-edge shock data on the stream surface at 50% flow from the casing (Fig. 5c) are confined to the near-stall throttle setting. The time locations of the discontinuities and the decrease in axial component across the discontinuity indicate a wave front nearer the perpendicular to the flow direction than to the axial direction.

Figure 6 places the shock location data on layouts of the cascades. The horizontal lines in the figure indicate axial positions of the measurement stations. Horizontal bars above these lines indicate the range of data taken at the near-stall throttle setting. A gap in the middle of the bar indicates a region of poor velocity definition during shock passage. Bars below the position lines, with similar gaps as appropriate, indicate data taken on the nominal operating line. Assuming that the blade locations do not move relative to the trigger, there must be substantial curvature of one or both wave fronts in the region forward of the LV coverage.

Figure 6 also shows the second shock in the cascade passage exit region where the flow compresses again, following supersonic expansion downstream of a throat. When the vehicle is throttled to the near-stall condition, this second shock disappears and the velocity components remain close to their immediate postshock values.

If the wave orientation is axial and the blade speed known, the discontinuity in the circumferential velocity components can be predicted. The stage design has some preswirl—8.4 deg on the 10% flow stream surface and 5.4 deg on the 30% flow stream surface—so that the measured circumferential components upstream of the leading-edge shock are realistic and must be included in the analysis. This analysis typically predicts 820 ft/s circumferential component discontinuity on the 10% flow stream surface, 670 ft/s on the 30% flow stream

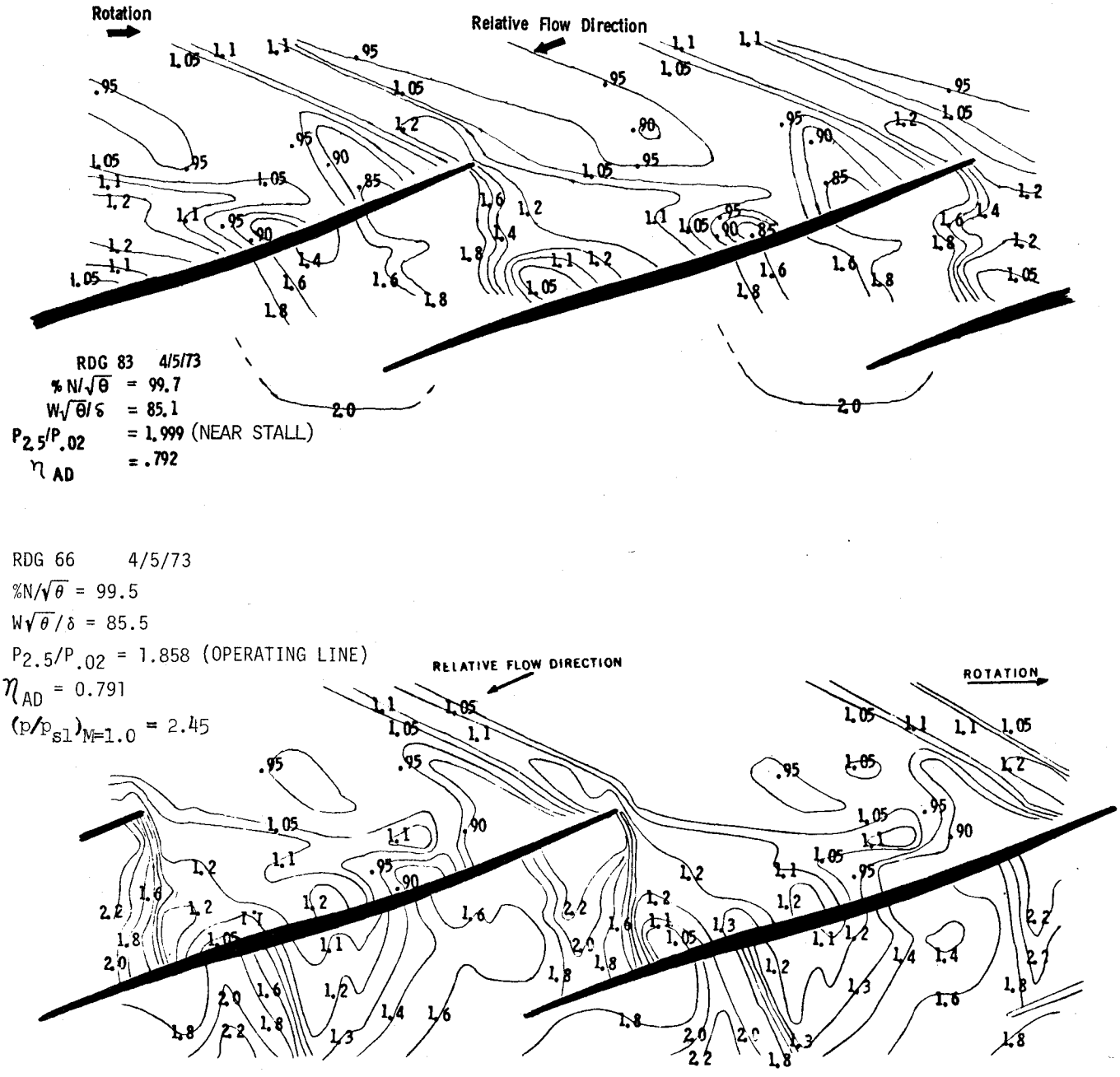

Fig. 7 Contour maps of casing static pressure—General Electric high tip speed (550 m/s).

surface. These predictions are higher than the measurements, particularly on the 10% flow stream surface.

The discrepancy between the predicted and measured discontinuities would be reduced if the axial wave front is not radial, but is actually skewed relative to a plane through the axis of rotation in order to allow some deflection radially outward. It is not clear how much skewness could be consistent with the geometry of this configuration. The idea of nonradial wave fronts will be explored in some detail later in this paper. Many observations are easier to understand when the influence of "S_2 surface obliquity" is included in an analysis.

Pressure contour data from high-frequency transducers on the casing are presented in Fig. 7. The orientation of the leading-edge shock across the cascade passage is very close to axial. Suction surface pressures substantially below upstream are shown. At the time these data were taken, it was hard to understand why pressure signals taken near midchord should show a sharp rise in pressure, followed by a rapid drop far ahead of the following airfoil pressure surface. Measurements of this type are responsible for a pressure "ridge" extending axially across the cascade passage. More recent thinking suggests that this "ridge" could be more evidence of the radial deflection hypothesis mentioned in connection with the predictions for circumferential velocity discontinuities. If the flow is being deflected radially across the shock, there must be some reflection at the casing, which might well be an overcompression and re-expansion.

Figure 7 also shows substantial response of the pressure surface pressure at midchord to throttling, even though these pressures are far below the expected sonic pressure level (2.45 times upstream static). Based on the static pressure levels, the midchord point is expected to lie in the "zone of silence" rather than the "zone of action" region for the downstream pressure. Unfortunately, the high-frequency transducers in the trailing-edge region did not give good signals for the near-stall test condition, so that the pressure patterns there cannot be compared.

This second example is used to show representative evidence that large oblique shock wave angles, approximating

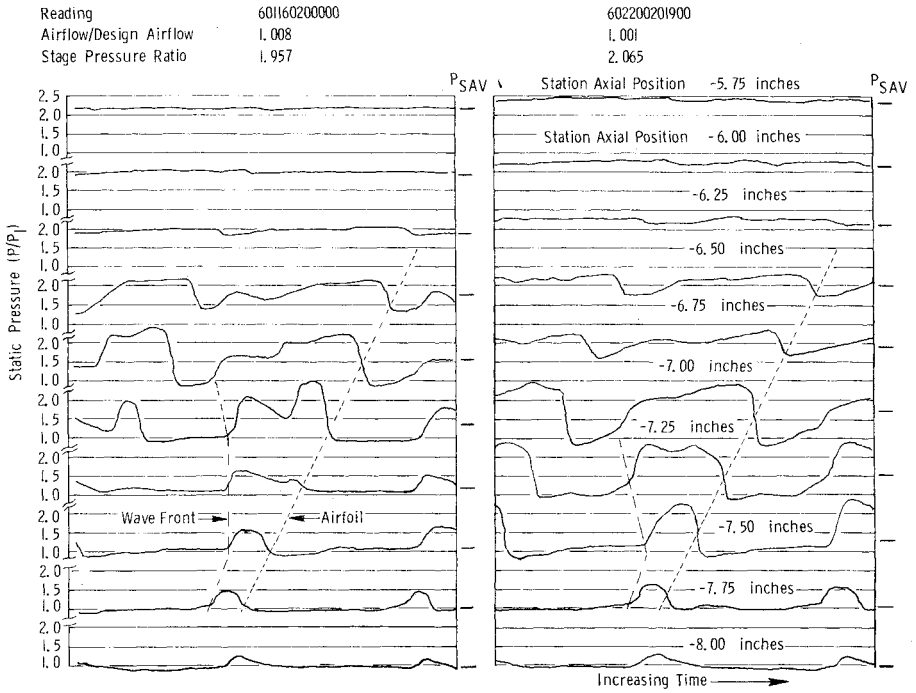

Fig. 8 Static-pressure transducer signals—USAF/APL HTF supersonic compressor stage.

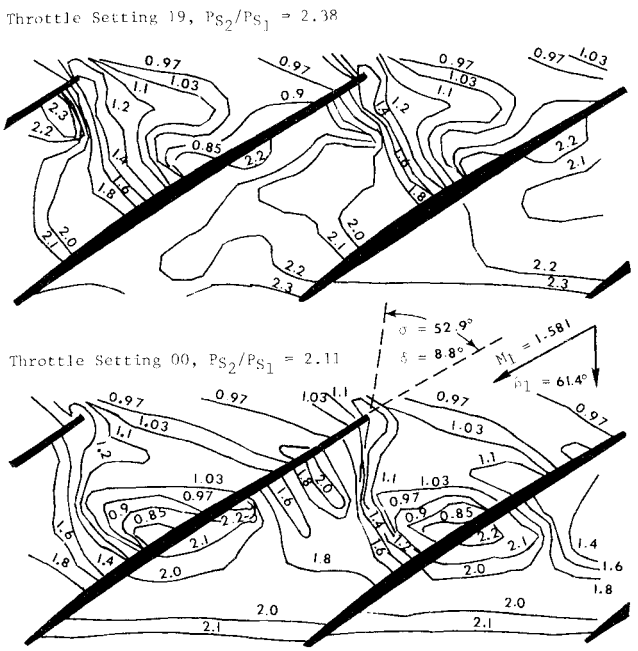

Fig. 9 Contour maps of casing static pressure—USAF/APL HTF supersonic compressor stage.

the maximum two-dimensional deflection, are observed in midannulus as well as on the casing. Reference 6 also shows LV evidence for axially oriented oblique shocks in midannulus.

Shock Structure Example 3—USAF High Through Flow Transonic Fan Stage

A. Wennerstrom of the U.S. Air Force has kindly made some experimental data available which complement the evidence of the first two examples. These data also served as the basis for theoretical studies into the shock structure.

Figure 8 presents the high-frequency casing pressure signals for this vehicle, reduced to the same pressure scale and adjusted for the time-average level at each location. Sharp pressure rises are identified with the shock wave front; sharp pressure drops are identified with passage of the airfoils. The airfoil location remains fixed as the vehicle is throttled, while the wave front moves upstream.

Figure 9 presents the processing of the time-varying pressure signals into pressure contour plots. The wave front orientation varies from essentially axial at the wide-open throttle condition to essentially normal near-stall. In each case, the pressure contours are shown normal to the suction surface. Since the wave orientation implies rather large stream deflection toward the suction surface, and near-sonic velocity downstream, subsonic conditions downstream of the shock in the wall-interaction region are clearly required. This vehicle also shows low-suction surface pressures for which no convincing explanation has been found.

An attempt has been made to check the pressure loading across the airfoil, indicated by the data of Figs. 8 and 9, against the momentum equivalent of the measured temperature rise. Assuming that the temperature rise from the discharge measurement rake elements nearest the tip is appropriate for the tip circulation, the blade pressure loading accounts for only 85% of the work input. The blade pressure loading also appears too small to support the measured pressure rise across the rotor.

No evidence of shock-type pressure rise is to be seen within the cascade passage, except across the leading-edge shock. The entire flow downstream of the leading-edge shock has a subsonic appearance, even though regions with pressure exceeding the 2.33 sonic level are exceptional.

This third example joins the first two in illustrating the predominance of rotor cascade flow patterns with the oblique shock wave angle for the leading-edge shocks approaching the angle corresponding to maximum deflection, and ranging from this type of angle toward the perpendicular to the flow direction.

Qualitative Model for the Supersonic Compressor Rotor Shock Structures

All the data that have been studied suggest that a qualitative view of the three-dimensional shock structure may be obtained by supposing the shock to be bounded on the upstream side by a surface generated from normal shocks across the cascade passage inlet along all stream surfaces of revolution, and on the downstream side by shocks with axial orientation.

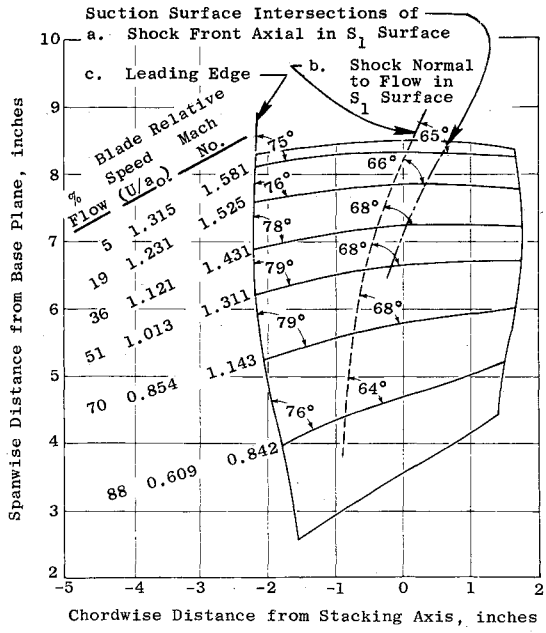

Fig. 10 Airfoil plan view showing S_1 surface intersections and shock loci—USAF/APL HTF supersonic compressor stage.

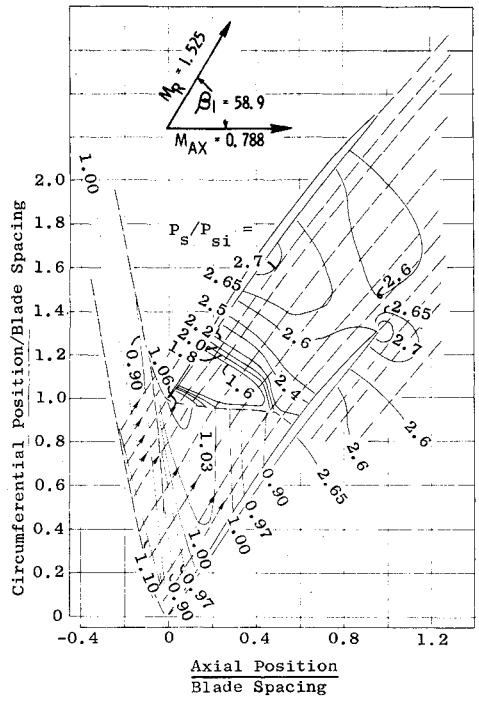

Fig. 11 Composite supersonic-subsonic flow pattern, 19% flow stream surface—USAF/APL HTF supersonic compressor stage.

This approach has been taken in Fig. 10. The figure shows a distorted plan view of the USAF/APL HTF airfoil, formed by twisting stream surface sections so that their chords lie in a plane. The stream surface intersections are retained during twisting and are included in the plan view. It is clear that the leading edge makes an oblique angle with all stream surfaces. The steep hub slope is primarily responsible for this obliquity in the inner half annulus. Near the airfoil tip, the obliquity comes from the constant radius casing and the spanwise variation of chord. Also shown in Fig. 10 are loci of normal and axial shock intersections with the suction surface. These loci are substantially more oblique to the stream surfaces than the leading edge.

Figure 10 has been prepared assuming that the shock on the suction surface extends toward the hub as far as the radius at which the relative Mach number is 0.8. Below the radius for sonic velocity, this shock need not extend all the way across the passage to the pressure surface, but could turn normal to the suction surface streamlines within the passage. Although Fig. 10 was prepared without the assistance of refined standoff distances, it seems appropriate to use the data from Ref. 23, which imply that the standoff distance should be 0.9% of the chord at 5% of the flow and 1.4% of the chord at 36% of the flow.

The shock equations obviously apply to the "S_2-oblique" shock. The momentum component in an S_2 surface parallel to the wave front is not disturbed. Conventional normal shock equations apply to the component perpendicular to the front. The result is a finite angle change for the S_2 surface streamlines as they cross the shock. How the local streamlines should be related to the streamlines in axisymmetric calculation procedures is not yet clear.

One consequence of this view of the flow pattern is that the turbomachine flowfield upstream of the shock is independent of the downstream flow, and may be analyzed without considering downstream conditions. Since many high-speed fan stages demonstrate pressure characteristics during throttling with little or no flow rollback, this feature is obviously realistic.

Supersonic Upstream Flowfield

Given the assumptions: 1) that a conventional turbomachine design procedure defines realistic meridional streamlines for the region close to the rotor tip and upstream of the portion of the leading-edge shock inside the cascade passage; and 2) that the upstream flow is independent of the downstream flow, it is possible to devise a cascade analysis for the supersonic relative flow on the surface of the revolution ("S_1 surfaces") defined by the meridional streamlines. The streamlines may be realistic even if the radial flow distribution is not.

The S_1 surface at 19% flow from the tip was selected for study in this investigation. Choice of this surface avoids modeling the interaction of the flow downstream of the shock, including an S_2 surface deflection, with the casing. On the other hand, the choice sacrificed ease of comparison of any analytical results with measured casing pressures.

The procedure used for supersonic flow analysis for the cascade includes several special features:

1) A model to introduce the influence of the blunt leading edge.

2) Variable lamina thickness for the effect of annulus convergence.

3) Method of Characteristics supersonic flow analysis, including imbedded shocks with their losses.

4) Momentum integral analysis for the flow through one cascade passage to determine the equivalent uniform flow far upstream.

5) Enforcement of periodicity by interpolating within the flowfield for properties to be transposed one period for use as inlet line definition.

Figure 11, a composite presentation of flowfield anlayses for the 19% flow S_1 surface of the USAF/APL HTF fan stage, makes use of the supersonic flow analysis for its upstream region. The passage shock must satisfy special requirements for matching the supersonic upstream flow to a quasisubsonic passage flow, and will be discussed later. An earlier version of the leading-edge model was described in a discussion to Ref. 12. The parameters to define it are obtained by interpolation in the field. Starting the process may require an arbitrary input for the flow upstream of the leading edge, such as the nominal upstream condition from the axisymmetric design. As a standard convention for analysis, the procedure chooses an inlet line parallel to the shock direction at the end of the subsonic zone around the stagnation point.

This line is extended to its intersection with the unique characteristic to upstream infinity, which is then followed as far as necessary, usually to an overlap with the second adjacent cascade passage. The nominal control surface for momentum integration starts at the intersection of a leading-edge shock with the streamline to the end of the subsonic zone for the first adjacent airfoil. The control surface proceeds upstream of the shock to the similar streamline for the second adjacent airfoil, then along that streamline to the periodic displacement of the starting point. Considerable flexibility may be allowed in the control surface without significantly affecting the validity of the momentum balance.

The airfoil, in this example, has a substantial reverse camber in the leading-edge region. In the analysis, the flow accelerates rapidly around the leading edge from the subsonic zone, then decelerates in the reverse camber region. Left running characteristics from the deceleration region coalesce and form the imbedded shock, which, in turn, is eventually absorbed into the leading-edge shock from the adjacent airfoil. Annulus convergence, such that the flow along any streamline sees decreasing streamtube area, decreasing Mach number in one-dimensional gasdynamics, is reponsible for the small static pressure increase along left running characteristics.

Results from the momentum balance analysis include:

1) Effective upstream flow angle and Mach number, as determined by leading-edge thickness, suction surface shape, and annulus convergence.

2) Effective axial Mach number and fraction of choke flow at the leading-edge plane.

3) Loss in total pressure from upstream infinity to the leading-edge plane due to shock structure.

Cascade Passage Shock Analysis

Some two-dimensional cascade analyses suggest the possibility of operating supersonic cascades with supersonic flow throughout. The design procedures described in Ref. 2, for example, call for all-supersonic flow. Experience, however, such as that reported in the discussion to Ref. 14, or the results of Figs. 3 and 7, shows that pressure surface pressures may stay well below the nominal pressure level for subsonic flow, and will still respond violently to changes in back pressure. This result appears to be incompatible with conventional two-dimensional cascade theories. Rather than attempt to use the usual analysis to develop passage shock shapes, the present investigation proceeded by idealizing observed shock shapes and exploring the theoretical implications of those idealized shapes.

The idealized shock shape in Fig. 11 includes the two main features of the experimental results: an axial orientation of the shock front for 80% of the cascade passage width, joining a normal front for the final 15% width to the suction surface. Analogous to the reflection at the suction surface of an oblique wave front when the flow can remain supersonic after additional deflection, it is supposed that the flow through the oblique portion of the wave should then see a subsonic transverse pressure gradient, which turns it back to parallelism with the suction surface. Analysis of the discontinuity across a shock front, which is oblique to the flow in both S_1 and S_2 surfaces, requires resolution of the upstream vector into a component perpendicular to the front, and components parallel to the intersections of the front with S_1 and S_2 surfaces. Then normal shock equations are applied to the perpendicular component. The downstream vector is reconstituted from the new normal component and the undisturbed tangential components. Figure 12 presents the results of this analysis, using S_2 surface obliquities deduced from Fig. 10. Downstream static pressures are compatible with measurements for the open throttle condition of Fig. 9. Downstream Mach numbers over most of the oblique shock range are low-supersonic, for which subsequent maximum allowable compression deflections are not more than 1-2 deg.

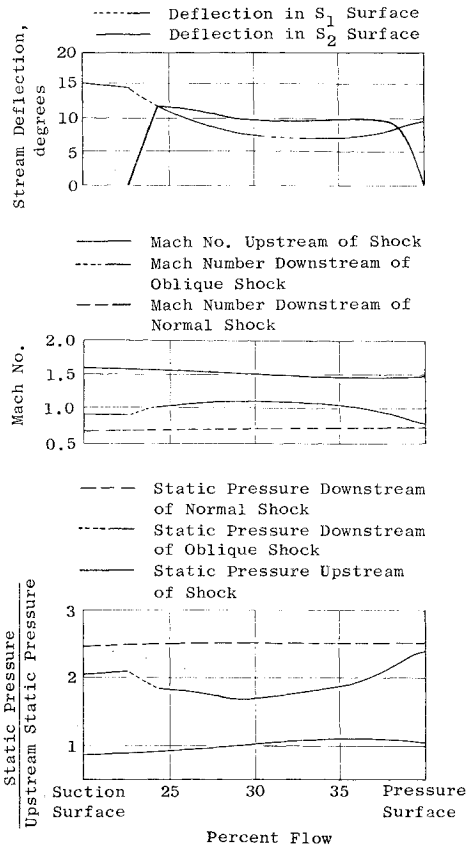

Fig. 12 Three-dimensional shock discontinuity analysis, shock oblique in S_2 surface, oblique in S_1 surface with transition to perpendicular near-suction surface, 19% flow stream surface—USAF/APL HTF supersonic compressor stage.

Internal Cascade Passage Flow Analysis

A final step in considering the flow through supersonic compressor rotors involves filling in the gap between a hypothetical shock structure and measured downstream flow conditions. Sometimes the gap filling involves clearly supersonic expansion and subsequent shocks, as in the low back pressure conditions of Figs. 4 and 7. In other cases, including the high back pressure condition of Fig. 9, an all-subsonic flow may seem suitable. As mentioned previously, the USAF/APL HTF stage has a substantial reverse camber near the leading edge. When the leading-edge model is applied to the reverse camber of the pressure surface, there is a significant convex curvature away from the flow direction for a sonic deflection. On a two-dimensional basis, this curvature calls for supersonic expansion. The fourth and fifth transducer signals from the low back pressure condition on Fig. 8 show evidence of this expansion. On stream surfaces more than 30% flow away from the tip, the locus of points terminating the subsonic zone moves away from the leading edge, leaving a substantial surface area open to the influence of downstream throttling. The following discussion of boundary conditions in the flow pattern downstream of the leading edge is, therefore, strictly applicable to this design alone and may require adjustment for other designs.

This investigation concentrated on a specific limited objective: to generate a basically subsonic flow pattern between the upstream parameters defined in Fig. 12, and a 0.74 Mach number far downstream estimated from overall vehicle measurements. The General Electric FLUXPLOT computer program described in Ref. 13 was used as a tool. This program is a relaxation solution of the equations of motion for subsonic inviscid flow, based on a Cartesian coordinate mesh. Its utility has been extended in ways particularly useful for this problem by using a tangent gas approximation for

Mach numbers greater than 0.95, which gives a plausible representation to about 1.25 Mach number when the pressure variations are primarily transverse to the flow directon due to streamwise curvature, and by allowing lamina thickness variations in both axial and circumferential directions. The user has up to 5000 mesh intersections available if they are needed for resolution in critical regions. About 1500 mesh intersections are usually enough to give satisfactory field definition.

Unless some unusual precautions are taken, the subsonic solution will not recognize the flow angle across the inlet line as a boundary condition, but will attempt to generate stream directions in essentially a fanwise manner over most of the passage width. Flow divergence away from the pressure surface can be encouraged if the lamina thickness decreases perpendicular to the wave front. At the same time, the lamina thickness on the upstream boundary is constrained so that the S_1 stream tube cross section area along any streamline can satisfy the A/A^* relationship to the specified downstream Mach number.

During the investigation, two additional special features appeared to be required in the lamina thickness distribution, if the resulting flowfield were to be plausible. First, observing on Fig. 9 that the suction surface pressure continues to increase slowly after the sudden increase through the wave front, the average lamina thickness on orthogonals to the flow in the region must be large enough to allow subsonic conditions over the entire passage width, including any pressure gradient from streamline curvature. The pressure field is only weakly dependent on the distribution of lamina thickness along such an orthogonal. Second, rapid lamina thickness increase is implied along the streamlines for flow adapting from the oblique shock deflection toward the suction surface to the subsonic condition parallel to the suction surface.

Figure 11 includes the streamline pattern and pressure contour field resulting from the subsonic passage solution. The main features conform quite well to expectation. In particular, the streamlines downstream of the shock do diverge from the pressure surface. The static pressure distribution on the downstream side of the shock makes the transition from a near-normal shock close to the pressure surface (oblique in the S_2 surfaces) with subsonic downstream conditions to the low-supersonic conditions near midstream, followed by a transition back to the normal shock and subsonic conditions near the suction surface. The steep pressure gradient for the pseudo-reflection of the shock in the subsonic field is present. There is a low-pressure region on the pressure surface in the 10% chord region, where the surface convexity calls for a transverse pressure gradient. Following the shock reflection, the flow decelerates steadily to the downstream pressure on the suction surface and to a level slightly above the downstream pressure on the pressure surface. The sonic static presure level is at 1.94 times upstream static pressure. The agreement between the subsonic presure field and the shock boundary condition is encouraging; it is expected that additional improvement is possible with more experimentation.

By analyzing the streamline curvatures of Fig. 11 along orthogonals to the flow, it is possible to estimate that the pressure surface pressure in the region between 10% and 15% of the chord should be approximately 20% of the upstream pressure below the pressure downstream of the shock in midpassage. It would be logical, therefore, to suggest an alternative analysis in which the strictly supersonic flow (retaining the model for the subsonic blunt edge region) is extended along the pressure surface to perhaps 20% chord, where it would be terminated through an S_1 normal shock. As mentioned earlier, the signals from transducers 4 and 5 from the low back pressure test condition suggest the separate existence of this S_1 normal shock.

The use of a lamina thickness, including a circumferential variation, appears to be unusual among literature references to cascade analyses. Some such features appear essential if this type of analysis is to represent the observations. Within the context of S_2 surface shock obliquities, it is clear that the variations in S_2 surface flow deflections ought to disturb the circumferentially uniform lamina thickness distribution that is appropriate upstream of the wave front. Moreover, to the extent that the flow tries to expand supersonically around the blunt edge and the subsequent reverse camber, very low-pressure surface pressures are generated, which may, in turn, induce radially outward flow from the sonic radius. The S_2 surface flow on the pressure surface must satisfy the equations of motion, with static pressures from continuity also meeting a force balance transverse to the flow.

Concluding Remarks

This author's experience suggests that conflict between experimental evidence and conventional theory occurs frequently during investigations into supersonic compressor behavior. The state of the art in instrumentation leaves some uncertainty in experimental results, such that observers may not accept them as motivation for re-examining their theories. This paper assumes that there is sufficient experimental evidence with satisfactory internal consistency to provide new insight into the phenomena. Table 1 summarized five features that appear regularly in the experimental evidence; representative experiments have provided illustrations.

Evidence for large shock wave angles comes from laser hologram photography, from the time relationships among pressure jumps at different axial positions as seen by high-frequency response transducers, from the time relationships among velocity discontinuities at different axial positions as seen by the laser velocimeter, and from the near-equality of axial velocity components on the two sides of the discontinuity as measured by the laser velocimeter. Of these methods of observation, holography probably provides the most dramatic display, and pressure signal results have been obtained on many different vehicles. The laser velocimeter results, however, are the most direct observation of a direction in which there is no momentum change. The laser velocimeter results also provide the most direct measurement of a wave velocity into an undisturbed fluid, and of the resulting momentum change. Recognition of these results should, therefore, figure prominently in any explanation of the shock behavior in transonic and supersonic compressors.

Identifying the S_2 surface obliquity of the shock structure seems to explain a significant part of anomalous shock behaviors. To the extent that the S_2 surface shock obliquity and other nonaxisymmetrical radial flow effects, such as centrifuging the pressure surface flow, dominate supersonic compressor flow patterns, two-dimensional cascade tests, and conventional two-dimensional cascade analyses present problems in interpolation.

Substantial progress has been achieved toward analytical representation of the realistic supersonic compressor flow through a combination of supersonic and subsonic analysis methods. Much remains to be done, especially in the direction of matching flow properties between stream surfaces. Since shock discontinuities are treated directly, and the supersonic and subsonic regions routinely contain more than 1000 mesh points, the system provides resolutions that are not easily obtained from other procedures under intensive development.

Acknowledgment

The author wishes to express appreciation to the General Electric Company and the U.S. Air Force for their encouragement during this investigation and for their permission to publish the material.

References

[1] Bilwakesh, K.R., Koch, C.D., and Prince Jr., D.C., "Final Report on Task II, Contract NAS3-11157 Performance of a 1500 Feet-per-second Tip Speed Transonic Fan Stage with Variable

Geometry Inlet Guide Vanes and Stator," NASA CR-72880, June 1972.

[2] Wright, L.C., Vitale, N.G., Ware, T.C., and Erwin, J.R., "High Tip Speed, Low Loading Transonic Fan Stage; Part I—Aerodynamic and Mechanical Design," NASA CR 121095, April 1973.

[3] Ware, T.C., Kobayashi, R.J., and Jackson, R.J., "High Tip Speed, Low Loading Transonic Fan Stage; Part III—Final Report," NASA CR 121263, Feb. 1974.

[4] Wuerker, R.F., Kobayashi, R.J., Heflinger, L.O., and Ware, T.C., "Application of Holography to Flow Visualization Within Rotating Compressor Blade Row," NASA CR 121264, Feb. 1974.

[5] Wisler, D.C., "Shock Wave and Flow Velocity Measurement in a High Speed Fan Rotor Using the Laser Velocimeter," ASME Paper 76-GT-49, *ASME Transactions, Journal of Engineering for Power*, April 1977, pp. 181-188.

[6] Dunker, R.V., Strinning, P.E., and Weyer, H.B., "Experimental Study of the Flow Field Within a Transonic Axial Compressor Rotor by Laser Velocimetry and Comparison with Through-Flow Calculations," ASME Paper 77-GT-28, *ASME Transactions, Journal of Engineering for Power*, April 1978, pp. 279-286.

[7] Gopalakrishnan, S. and Bozzola, R., "A Numerical Technique for the Calculation of Transonic Flows in Turbomachinery Cascades," ASME Paper 71-GT-42, March 1971.

[8] Gopalakrishnan, S. and Bozzola, R., "Computation of Shocked Flows in Compressor Cascades," ASME Paper 72-GT-31, March 1972.

[9] Gopalakrishnan, S. and Bozzola, R., "Numerical Representation of Inlet and Exit Boundary Conditions in Transient Cascade Flow," ASME Paper 73-GT-59, *ASME Transactions, Journal of Engineering for Power*, Oct. 1973, pp. 340-344.

[10] McDonald, P.W., "The Computation of Transonic Flow through Two-Dimensional Gas Turbine Cascades," ASME Paper 71-GT-89, March 1971.

[11] Gliebe, P.R., "Coupled Inviscid/Boundary-Layer Flow-Field Predictions for Transonic Turbomachinery Cascades," *Transonic Flow Problems in Turbomachinery*, T.C. Adamson and M.F. Platzer, eds., Naval Postgraduate School, Monterey, Calif., MICH-16-PU, Feb. 1976, pp. 434-452.

[12] York, R.E. and Woodard H.S., "Supersonic Cascades—An Analysis of the Entrance Region Flow Field Containing Detached Shock Waves," ASME Paper 75-GT-33, *ASME Transactions, Journal of Engineering for Power*, April 1976, pp. 247-257.

[13] Prince Jr., D.C., "Evaluation of Compressibility Effects by the Compressible Fluxplot Computer Program," GE TIS Rept. R66FPD270, Sept. 1966.

[14] Gostelow, J.P., "Review of Compressible Flow Theories for Airfoil Cascades," *ASME Transactions, Journal of Engineering for Power*, Oct. 1973, pp. 281-292, discussion by D.C. Prince Jr., *Journal of Engineering for Power*, Jan. 1974., pp. 77-79.

[15] Epstein, A.H., Kerrebrock, J.L., and Thompkins Jr., W.T., "Shock Structure in Transonic Compressor Rotors," *AIAA Journal*, Vol. 17, April 1979, pp. 375-379.

[16] Delaney, R.A. and Kavanagh, P., "Transonic Flow Analysis in Axial-Flow Turbomachinery Cascades by a Time-Dependent Method of Characteristics," *ASME Transactions, Journal of Engineering for Power*, July 1976, pp. 356-364.

[17] Lichtfuss, H.J. and Starken, H., "Supersonic Exit Flow of Two-Dimensional Cascades," ASME Paper 72-GT-49, March 1972.

[18] Lichtfuss, H.J. and Starken, H., "Supersonic Cascade Interaction," ASME Paper 74-GT-76, March 1974.

[19] Simon, H., "A Contribution to the Theoretical Examination of the Flow Through Plane Supersonic Deceleration Cascades and Supersonic Compressor Rotors," ASME Paper 73-GT-17, March 1973.

[20] Hantman, R.G., Mikolajczak, A.A., and Camarata, F.J., "Application of a Two-Dimensional Supersonic Passage Analysis to the Design of Compressor Rotors," ASME Paper 74-GT-97, March 1974.

[21] Erwin, J.R. and Vitale, N.G., "The Radial Outflow Compressor," *Advanced Centrifugal Compressors*, published by ASME, 1971, p. 56.

[22] Fruehauf, H.H., "Spatial Supersonic Flow Through Annular Cascades," ASME Paper 75-GT-113, March 1975.

[23] Holder, D.W. and Chinneck, A.; "The Flow Past Elliptic-Nosed Cylinders and Bodies of Revolution in Supersonic Air Streams," *Aeronautical Quarterly*, Vol. 4, Feb. 1954, pp. 317-340.

[24] Lighthill, M.J., *Higher Approximations in Aerodynamic Theory*, Princeton Aeronautical Paperbacks No. 5, Princeton University Press, 1960, Sec. E5.